Supersonic Business Jet Design using a Knowledge-Based Genetic Algorithm with an Adaptive, Unstructured Grid Methodology

Hyoung-Seog Chung*
Seongim Choi†
Juan J. Alonso‡
Stanford University, Stanford, CA 94305

In the design of supersonic low-boom aircraft, it is important to balance the aerodynamic performance and sonic boom requirements in a way that represents the best compromise for the overall design. Since the ground sonic boom is typically not a smooth function of the design variables and may actually contain multiple local minima, it is important to select an optimization algorithm that is able to cope with this kind of design space. In this work, we study the use of Kriging approximation models for both boom and performance and use them in conjunction with genetic algorithm techniques to investigate the computational cost and characteristics of such an approach for the design optimization of a low-boom supersonic business jet (SBJ). Direct use of genetic algorithms with high-fidelity CFD analysis tools has been limited by the inherently large computational cost of genetic algorithms (GAs). The use of computationally inexpensive approximation models in lieu of high-fidelity CFD greatly improves the robustness and efficiency of the design process for searches in relatively large design spaces. In order to improve the performance of this method, a new hybridization strategy that combines a GA with gradient information is proposed and its improved convergence rate is demonstrated. Regardless, the proposed procedures still require a large number of evaluations of the flow and boom patterns for different points in the design space. For this purpose we have built two automated Euler analysis tools that use a CAD-based geometry engine, and both multiblock-structured and unstructured, adaptive meshing techniques (they are named QSP107 and QSP-UA respectively). QSP-UA, has been developed to handle the geometric detail of the complete configuration including wing, fuselage, nacelles, diverters, empennage, etc., and to provide accurate performance and boom data. Results of sample test problems, and a 15-dimensional design case are presented and discussed.

1. Introduction

FOR decades, the development of economically and environmentally acceptable supersonic aircraft has been identified as a key step toward the next generation of aviation history that could improve many aspects of human life and foster economic growth. The partial consensus view of prospective manufacturers of supersonic aircraft is that the supersonic business jet (SBJ) is a near-term-realizable class of vehicle having significant economic potential and with an estimated market of at least 200 aircraft over a 10-year period.[1] The key technology barrier for this class of aircraft is the elimination, or reduction to acceptable levels, of the sonic boom for flight over land while guaranteeing the challenging performance requirements of the other major disciplines. This essentially means that all major disciplines including aerodynamics, structures, stability and control, mission, and propulsion should be taken into account from the early stages of design process; therefore, boom reduction must be considered as an additional aspect of the MDO problem.

MDO methods, particularly those based on high-fidelity analyses, greatly increase the computational burden and complexity of the design process.[2–5] For this reason, high-fidelity analysis software typically used in single discipline designs may not be suitable for direct use in MDO.[3,6] Faced with these problems, the alternative of using approximation models of the actual analysis software has received increased attention in recent years.

The Kriging technique, developed in the field of geostatistics, has been recognized as an alternative to the traditional polynomial function-based Response Surface method in generating approximation models of computationally expensive CFD analyses. In theory, it is able to interpolate sample data and to model functions with multiple local extrema.[8,9] Using variations of the method of design of experiments (DOE), the Kriging model can efficiently represent global trends of design space.

Once a approximation model is generated, it can easily be used to search for optimum combinations

*Doctoral Candidate, AIAA Member
†Doctoral Candidate, AIAA Member
‡Assistant Professor, Department of Aeronautics and Astronautics , AIAA Member

of design variables within the design space. Since the Kriging model can represent multimodal functions with relatively low computational cost, it would be reasonable to choose a global optimization scheme as the optimizer.

Genetic algorithms (GAs) are search algorithms based on the mechanics of natural selection where the encoded design variables (or so-called genes) are manipulated using genetic-like operators such as selection, crossover and mutation to generate new populations of candidate design points. One of the biggest advantages of GAs is their robustness. Since GAs do not require sensitivity information, they can be applied to realistic design environments where discontinuities, multimodality and noisy responses may exist. They also have considerable advantages for multiobjective design problems to obtain Pareto optimal sets. A major drawback of the GA approach is that it requires many generations to locate the global optimum point. Because of this reason, the utilization of GAs in high-dimensional design spaces with high-fidelity analyses has been impractical, if not impossible. Therefore, the use of accurate and efficient approximation models with the ability to simulate the multimodal nature of some objective functions can help decrease the cost in realistic design problems. Goldberg introduced the idea of using approximation models with GAs under the name of "knowledge-based GAs.[10]" In this work, and starting from this strategy, a new hybridization approach that combines GAs with the available gradient information has been proposed and its improved convergence rate has been demonstrated. We have also studied the use of Kriging models as gradient estimators for CFD-based GAs in the low-boom SBJ design problem.

There have been many difficulties in analyzing sonic boom signatures using CFD methods. These problems are associated with issues of mesh resolution, artificial dissipation formulation, two-dimensional versus three-dimensional signature propagation methods, and the exact formulation of these propagation procedures. The fundamental difficulty in predicting sonic booms accurately is that a near-field pressure signature must be obtained sufficiently far from the aircraft so that the pressure disturbance can be modeled using geometrical acoustics. Given the dissipative nature of CFD methods, very high mesh resolution is required between the lower surface of the aircraft and the near-field location (typically 1-5 body lengths below the aircraft) leading to extremely large meshes even for inviscid calculations. This mesh resolution/distribution issue is tightly coupled with the fact that complex geometry representation (full configurations including nacelles, diverters, etc.) is typically necessary in the shaping of low sonic boom aircraft. Complete configurations also require higher mesh resolution for capturing shock and expansion waves around the aircraft.

Unstructured meshes are ideally suited to address these meshing issues since they can easily conform to arbitrarily complex aircraft shapes and they can be locally adapted to capture the relevant physical phenomena. This adaptive mesh refinement strategy can improve computational efficiency in the presence of finite computing resources.

An automated, nonlinear integrated boom analysis tool, QSP-UA, which incorporates a routine for adaptive unstructured mesh generation, a three-dimensional Euler flow solver, and a boom propagation procedure has been developed and is used here for the computation of accurate near-field and ground pressure distributions. This tool is used for collecting sample data for the creation of approximation models.

In this paper, our intention is to explore the applicability and efficiency of using genetic algorithm techniques in conjunction with approximation models representing response functions with multiple local minima and sharp discontinuities in the multidimensional design optimization of a low-boom supersonic business jet configuration. The goal of this multiobjective design optimization problem is to reduce the sonic boom signature at the ground by modifying the aircraft configuration parameters while preserving or improving aerodynamic performance.

2. Overview of Kriging Method

The Kriging technique uses a two component model that can be expressed mathematically as

$$y(\boldsymbol{x}) = f(\boldsymbol{x}) + Z(\boldsymbol{x}), \tag{1}$$

where $f(\boldsymbol{x})$ represents a global model and $Z(\boldsymbol{x})$ is the realization of a stationary Gaussian random function that creates a localized deviation from the global model.[12] If $f(x)$ is taken to be an underlying constant,[9] β , Equation (1) becomes

$$y(\boldsymbol{x}) = \beta + Z(\boldsymbol{x}), \tag{2}$$

which is used in this paper. The estimated model of Equation (2) is given as

$$\hat{y} = \hat{\beta} + \boldsymbol{r}^T(\boldsymbol{x})\boldsymbol{R}^{-1}(\boldsymbol{y} - \boldsymbol{f}\hat{\beta}), \tag{3}$$

where $\boldsymbol{y}$ is the column vector of response data and $\boldsymbol{f}$ is a column vector of length n_s which is filled with ones. $\boldsymbol{R}$ in Equation (3) is the correlation matrix which can be obtained by computing $R(\boldsymbol{x}^i, \boldsymbol{x}^j)$, the correlation function between any two sampled data points. This correlation function is specified by the user. In this work, the authors use a Gaussian exponential correlation function of the form provided by Giunta, et al.[7]

$$R(\boldsymbol{x}^i, \boldsymbol{x}^j) = \exp\left[-\sum_{k=1}^{n} \theta_k |\boldsymbol{x}_k^i - \boldsymbol{x}_k^j|^2\right]. \tag{4}$$

The correlation vector between $\boldsymbol{x}$ and the sampled data points is expressed as

$$\boldsymbol{r}^T(\boldsymbol{x}) = [R(\boldsymbol{x}, \boldsymbol{x}^1), R(\boldsymbol{x}, \boldsymbol{x}^2), ..., R(\boldsymbol{x}, \boldsymbol{x}^n)]^T. \quad (5)$$

The value for $\hat{\beta}$ is estimated using the generalized least squares method as

$$\hat{\beta} = (\boldsymbol{f}^T \boldsymbol{R}^{-1} \boldsymbol{f})^{-1} \boldsymbol{f}^T \boldsymbol{R}^{-1} \boldsymbol{y}. \quad (6)$$

Since $\boldsymbol{R}$ is a function of the unknown variable $\boldsymbol{\theta}$, $\hat{\beta}$ is also a function of $\boldsymbol{\theta}$. Once $\boldsymbol{\theta}$ is obtained, Equation (3) is completely defined. The value of $\boldsymbol{\theta}$ is obtained by maximizing the following function over the interval $\boldsymbol{\theta} > \mathbf{0}$

$$-\frac{[n_s \ln(\hat{\sigma}^2) + \ln|\boldsymbol{R}|]}{2}, \quad (7)$$

where

$$\hat{\sigma}^2 = \frac{(\boldsymbol{y} - \boldsymbol{f}\hat{\beta})^T \boldsymbol{R}^{-1} (\boldsymbol{y} - \boldsymbol{f}\hat{\beta})}{n_s}. \quad (8)$$

In order to construct a Kriging approximation the only data required are the function values at a number of pre-specified sample locations. For many computational methods, secondary information such as gradient values may be available as a result of the analysis procedure. Alternatively, the gradient vector can be computed with very little additional cost, as is the case in the adjoint method.[4] Gradient information is usually well cross-correlated with the function values and thus contains useful additional information. The efficiency and accuracy of Kriging models can be greatly improved by incorporating these secondary function values.[13] This technique, known as the Cokriging method, has been investigated and validated in our previous work.[14,15]

3. Advanced Genetic Algorithms

3.1 Multiobjective Genetic Algorithms

Many real-world optimization problems, especially in MDO situations, require the simultaneous optimization of possibly conflicting multiple objectives: this approach is often referred to as *multiobjective optimization*. Unlike single-objective optimization where only one optimal solution is pursued, a typical multiobjective optimization problem produces a set of solutions which are superior to the rest with respect to all objective criteria, but are inferior to other solutions in one or more objectives. These solutions are known as Pareto optimal solutions or non-dominated solutions. None of the solutions in the Pareto optimal set is absolutely better than any others with respect to all of the objectives being considered; therefore, any one of them is an acceptable solution. Once the set of optimal solutions is identified, it is left to the designer to choose one solution out of the many possible ones.

A genetic algorithm can use this dominance criteria in a straightforward fashion to drive the search process toward the Pareto front. Due to the unique features of GAs, which work with a population of solutions, multiple Pareto optimal solutions can be captured in a single run. This is the primary reason that makes GAs ideally suited for multiobjective optimization.

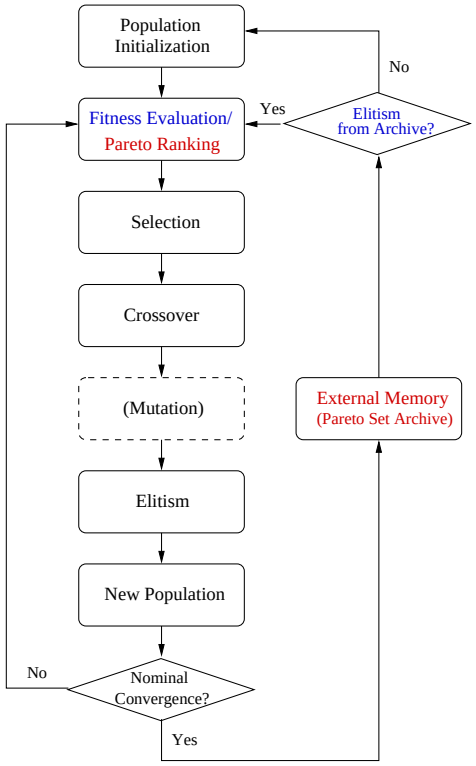

Fig. 1 Flow Chart for Multiobjective GA

A recent study by Coello[16] proposed a micro-GA-based multiobjective optimization that uses an external file of non-dominated vectors found in previous generations to accelerate the multiobjective optimization process. The method implemented an additional elitism strategy and an adaptive grid-type technique to accelerate the convergence and to keep the diversity in the Pareto front. The Micro-GA algorithm is a specialized GA that works with a very small population size of usually 3-6 and a reinitialization step. Studies[16,17] have shown that micro-GAs achieved a faster convergence rates than simple GAs. In the present research, some of the ideas of Coello's work have been adapted to a single objective micro-GA algorithm along with the traditional Goldberg's Pareto ranking approach in order to develop an efficient and robust design framework. The authors have modified a micro-GA algorithm originally developed by Carroll.[18]

The procedure is illustrated in Figure 1. First, a random population is generated and their objective values are calculated as in the original micro-GA. Then, to ensure that all the non-dominated individuals have same level of reproductive potential, Goldberg's non-dominated sorting procedure is implemented. Therefore, the fitness level of each individual is determined based on the non-domination criterion rather than the

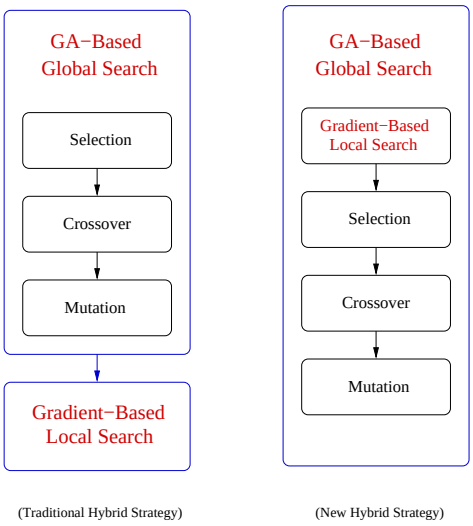

Fig. 2 New Hybrid GA Strategy

objective function value itself.

Based on the rank of non-dominance, the population goes through the usual operations of micro-GA, namely selection and crossover, and check to see if the nominal convergence among the population points has been reached. If the problem is not converged, the algorithm returns to the function evaluation and non-dominance ranking steps for the new generation, otherwise it continues on to the reinitialization step.

Two types of elitism are implemented in the reinitialization step. The first type carries on the best solutions from the previous nominal convergence stage. This is the same elitism strategy used in the single objective micro-GA. The second type involves the storing of non-dominated vectors produced from each cycle of micro-GA to an external file and inserting some of the best solutions generated so far in the reinitialized population for the micro-GA. This process is applied at regular intervals to improve the non-dominated solutions by getting closer to the true Pareto front or by achieving a better distribution.

3.2 Gradient Enhanced Micro-GA

The convergence history of GAs can be characterized as having a fast portion during the early stage of a run followed by very slow progress in the later stages. This means that GAs work reasonably well up to a near-optimal solution but they consume an unacceptable number of generations and function evaluations to attain the real optimum. Because of this, an obvious improvement to the GA is to take advantage of the characteristics of gradient-based optimizers after a certain level of convergence has been achieved by the GA. The strategy of traditional hybridization is to obtain some of the candidates for the optimal solution from the GA and to then apply a gradient-based optimizer starting from those points to accelerate the convergence to the optimal point. This approach can be seen in Figure 2 below.

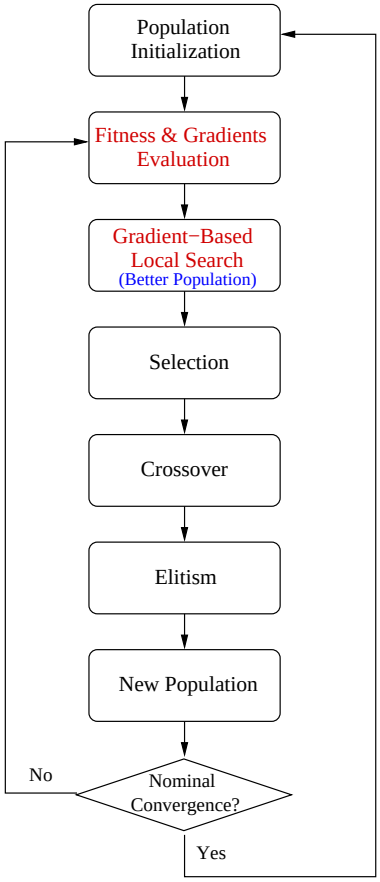

Fig. 3 Flow Chart for Gradient-Enhanced Micro-GA

A new strategy of hybridization using gradient information is proposed in the present research. Instead of combining a gradient-based optimizer at the end of a GA run, the proposed method implements the gradient information at every generation of the GA. The schematic procedure of the method is shown in Figure 3. The only difference between the new hybrid micro-GA and the original micro-GA is that all the individuals in a population are updated or improved using the steepest descent method with the gradient information available *before* they go through the processes of selection and crossover at each and every generation. That is, the hybridization is achieved by inserting a gradient-based optimizer (steepest descent method) at the GA operator level. This results in more closely combined hybridization procedures.

3.3 Approximation Model based micro-GA

Once fairly accurate global approximation models are constructed with computationally efficient techniques such as the Kriging or Cokriging methods, combining them with GAs becomes an obvious choice to overcome the computational burden presented by directly-coupled GA methods. Since the computational cost of estimating the objective function through the approximation models is trivial, the slow convergence rate of GAs leading to many generations and

function evaluations to get to the optimal solution does not matter any more. If the approximation model is accurate enough, it can even provide auxiliary information such as gradients to accelerate the process even further. In addition, GAs are a more suitable approach than gradient-based methods for use with approximation models that can support multimodal functions.

The approximation model itself can benefit from the use of a direct GA by recycling the rich dataset produced with each population. The mutual benefits of combining these two methods can provide the efficient and robust design framework necessary in MDO. Yet another way of using approximation models for accelerating the GA process is to use them as a gradient estimators to provide the necessary gradient information for the hybrid micro-GA proposed in the previous section. Note that even though adjoint methods can provide gradient information cheaply and efficiently, the derivation of the adjoint equations and boundary conditions can not be carried out for arbitrary cost functions. In addition, an adjoint code implementation might take months of validation. Therefore, the approximation models can be a useful and inexpensive alternative for computing the gradients.

4. Test Problem : Low-Boom Supersonic Business Jet (SBJ) Design

The design problem in question involves the simultaneous ground boom and drag minimization of a supersonic business jet wing-body-tail (and possibly nacelles with the unstructured method) configuration at a specified lift coefficient, $C_L = 0.07104$, which corresponds to a cruise weight of $100,000$ lbs at a cruise altitude of $50,000$ ft. The wing reference area is $1,032\ ft^2$. The free-stream flow conditions were fixed at $M_\infty = 2.0$. The aircraft geometry and flow conditions were parameterized directly in CAD using 108 design variables.[19] The list of geometric design variables for the 15-dimensional design problem which we will describe later is given below:

x_1= wing position along fuselage
x_2= wing dihedral angle
x_3= wing sweep angle
x_4= wing aspect ratio
x_5= wing leading edge extension
x_6= upper fuselage radius at 12.50% of fus. length
x_7= upper fuselage radius at 18.75% of fus. length
x_8= upper fuselage radius at 25.00% of fus. length
x_9= upper fuselage radius at 31.25% of fus. length
x_{10}= upper fuselage radius at 37.50% of fus. length
x_{11}= lower fuselage radius at 12.50% of fus. length
x_{12}= lower fuselage radius at 18.75% of fus. length
x_{13}= lower fuselage radius at 25.00% of fus. length
x_{14}= lower fuselage radius at 31.25% of fus. length
x_{15}= lower fuselage radius at 37.50% of fus. length

The wing planform for this configuration was designed with experience from our previous supersonic work to have a portion with a subsonic leading edge followed by an outboard panel with a supersonic leading edge. This helps increase the span to achieve better low-speed performance at a small cost in cruise performance. The airfoil sections for the outboard portion of the main wing and the horizontal tail were chosen to be simple biconvex airfoils of varying thickness, while an RAE2822 was used for the inboard part of the main wing with a subsonic leading edge. Fuselage aft-mounted nacelles are included in the baseline design, although their presence was only modeled in the optimization results based on our unstructured analysis environment.

A CFD/boom analysis of the two objective criteria considered in this study yields values for the baseline design of an inviscid coefficient of drag, $C_D = 0.010046$ and an initial shock pressure rise, $\Delta p = 0.91157$psf respectively. The performance of the baseline configuration at this low C_L condition is admittedly low so that we can analyze the speed with which the proposed algorithms approach the Pareto fronts. We are currently repeating the optimizations presented in this paper with a baseline design that has been thoroughly optimized (for aerodynamic performance alone) using our multiblock adjoint design program.[19] All improvements in either or both of these criteria are measured against the value for this baseline configuration.

5. Design Tools

In order to develop Kriging and Cokriging approximation models, a large number of CFD computations for different geometries must be carried out automatically. For this purpose, we have developed two separate nonlinear integrated boom analysis tools, QSP107 and QSP-UA, that can provide both ground boom and aerodynamic performance information by simply changing a small set of configuration variables that are provided in an input file. QSP107 is our structured-mesh analysis suite, while QSP-UA relies on an unstructured adaptive tetrahedral flow solver.

5.1 QSP107

QSP107 is a nonlinear integrated tool for both sonic boom prediction and aerodynamic performance analysis based on fully nonlinear CFD. This tool couples the multiblock Euler and Navier-Stokes flow solver for structured mesh, FLO107-MB,[20] to a CAD-based geometry kernel and a mesh perturbation procedure for efficient mesh regeneration, and to the PC Boom software for far-field propagation developed by Wyle Associates.[22] A flowchart of the automated analysis process can be seen in Figure 5.

The procedure starts with a CAD-based geome-

try generation module called AEROSURF that uses a parametric CAD model to automatically generate the necessary surface meshes to describe the configuration in question.[19] This geometry module is based on a parametric aircraft description with 108 design variables of which only a small subset (either two or fifteen) are chosen for our optimization applications. AEROSURF relies on the CAPRI CAD interface of Haimes[19,23] to provide access to a number of parametric CAD software programs including Pro/Engineer, CATIA V5, SolidWorks, and I-DEAS. Parametric aircraft models of arbitrary complexity can be created and used within this environment, thus automating some of the most complicated geometry manipulations that are the heart of any high-fidelity design procedure.

The surface meshes generated by AEROSURF, together with an initial multiblock mesh that is generated using the Gridgen software[24] are passed to a mesh perturbation routine called Meshwarp that can handle arbitrary configurations and generate volume meshes corresponding different surface geometries. As constructed, the meshes have higher resolution in the areas where shock waves and expansions are present below the aircraft, and the grid lines are slanted at the Mach angle to maximize the resolution of the pressure signature at a distance of the order of one to three fuselage lengths below the aircraft. The user may specify the location of an arbitrary cylindrical surface where the near-field signature is extracted from the multiblock flow solution and then provided as an input to a modified version of PC Boom which propagates a full three-dimensional signature along all rays that reach the ground. This allows for the calculation of arbitrary cost functions (not only ground-track initial overpressure) that may involve weighted integration of the complete sonic boom footprint. In this work, however, only the ground track overpressure has been considered.

The flow solver, FLO107-MB, combines advanced multigrid procedures and a preconditioned explicit multistage time-stepping algorithm which allows full parallelization. Because of the advanced solution algorithms and parallelization, the integrated tool provides fully nonlinear simulations with very rapid turnaround time. Using typical meshes with over 3×10^6 mesh points we can obtain a complete flow solution and ground signature in around 7 minutes, using 16 processors of a Beowulf cluster made up of AMD AthlonXP 2100 processors. In this work, QSP107 has been used repeatedly to generate Kriging and Cokriging approximation models and it has also been directly coupled with a genetic algorithm for the design optimization process.

5.2 QSP-UA

QSP107 imposes some limitations on the magnitude of the shape perturbations that can be handled since it relies on a single multiblock mesh (generated prior to the start of the design procedure) and a mesh perturbation routine. If the surface perturbations are large, the mesh perturbation procedure may fail.

In order to overcome these limitations when exploring very large design spaces, QSP-UA includes and unstructured adaptive mesh generation/perturbation capability based on the Centaur mesh generation software.[25] As in QSP107 the procedure is fully automated from the specification of the design variables for a given configuration to the computation of both the coefficient of drag and the ground boom overpressures.

This tool integrates the three-dimensional Euler flow solver AirplanePlus which is a C++ implementation of the original AIRPLANE solver of Jameson[28] with an agglomeration multigrid strategy, and MPI-based parallelization, and the ability to solve the Reynolds-Averaged Navier-Stokes (RANS) equations on unstructured tetrahedral meshes. As in QSP107, the unstructured adaptive solution is passed to the PC Boom software to propagate the near-field pressure distributions to the ground.

QSP-UA functions in a manner that is similar to QSP107 except for the surface and volume mesh generation and the actual flow solver. It also uses AEROSURF to provide the surface definition of the aircraft geometry. With the input of this CAD-defined geometry and pre-defined far-field boundaries, Centaur uses an advancing-front method to generate both surface and volume meshes.

Tetrahedral Mesh Generation

The current methods available for the generation of tetrahedral meshes[29–31] are typically based on either advancing front or Delaunay triangulation ideas. In our work, the advancing-front method[26] in the form of the Centaur software is used for mesh generation and perturbation.

As mentioned above, the Centaur software is used in our work to construct meshes for aircraft configurations and to enhance grid quality through automatic post-processing. Only the fine meshes need to be explicitly constructed since our multigrid algorithm is based on the concept of agglomeration and, therefore, coarser meshes are obtained automatically.

Figure 4 shows a typical, unadapted, tetrahedral mesh around our baseline configuration. The figure contains only the surface triangles of the aircraft and the symmetry plane for visualization purposes.

Mesh Adaptation Procedures

Once an initial solution has been computed on the tetrahedral mesh, the grid needs to be locally adapted

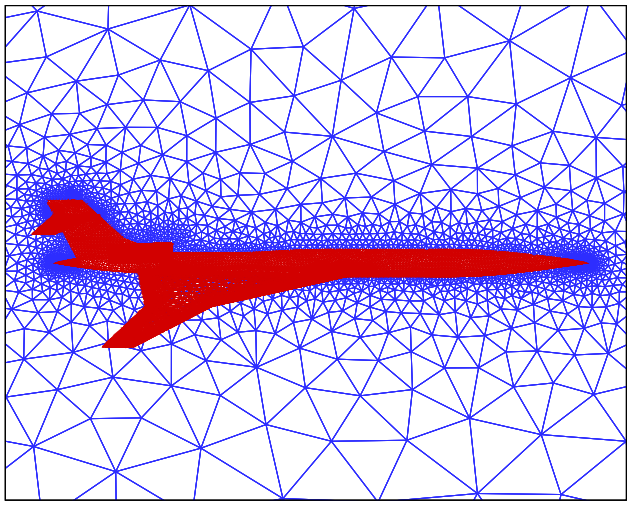

Fig. 4 Unstructured tetrahedral surface mesh around a low-boom aircraft

to better capture specific features with higher accuracy at lower cost. This can be achieved through a more optimal distribution of grid points for each computed solution: unstructured tetrahedral elements are well suited for cell adaptation. For the cases that we have studied, coarsening has only a minor performance impact in steady-state calculations and is omitted in this study.

The adaptation procedure utilizes h-refinement or subdivision techniques. For each edge that is flagged by the error estimation technique, new mesh nodes are inserted at the midpoint. For boundary edges, these points are repositioned onto the splined surface which defines the original geometry from the CAD package. The current post-adaptation grid-improvement scheme employs face and edge swapping. Undesirable shape measures are investigated and new local tetrahedral configurations with more desirable shape measures are selected.

The adaption procedure is, of course, recursive, and it proceeds until a certain level of error has been achieved or a maximum number of refinement levels has been accomplished. Figure 6 (a) shows the mesh after the first adaptation. The selection of the initial mesh resolution is important to capture the underlying pressure gradients. Since boom prediction is the driving feature to be captured in this study and shock angle is relatively predictable, uniform local adaptation (mainly in the region under the aircraft) is performed after the initial mesh is generated. Figure 6 (b) shows the solution-adapted mesh after two adaptation steps. Typically, four consecutive adaption cycles are performed automatically starting with the initial mesh to reach the necessary solution quality.

The most popular refinement options for fluid-flow problems are heuristically derived gradient-based criteria, which involve a single or multiple physical flow variables. The gradient of pressure can be used to identify inviscid flow features. But in sonic boom prediction problems the pressure gradient in the near field is as important as in the neighborhood of the aircraft. In addition, the direction of the gradient should be taken into account as well. In this study, a pre-specified range of velocity gradient magnitudes which are projected onto the direction of the local pressure gradient work successfully to predict the shock location and to capture small pressure gradients in near-field.

In the following expression for the adaption criterion $\mathbf{V}$ is the velocity vector, c is speed of sound and $\triangle x$ is required minimum edge length.

$$\epsilon^{'} = \frac{\mathbf{V}}{c} \cdot \frac{\nabla p}{|\nabla p|} \tag{9}$$

Numerical experiments[32] indicate that the modification of the previous equation to include a local mesh length-scale such as:

$$\epsilon = \frac{\mathbf{V}}{c} \cdot \frac{\nabla p}{|\nabla p|} \triangle x \tag{10}$$

produces a more effective refinement criterion for shock/expansion flows. This is partially due to the fact that while the simple gradient-based criteria decreases in magnitude as the mesh is refined in smooth regions of flow, it remains approximately constant in the vicinity of shock waves, since the shock wave profile steepens as the mesh is refined, and the jumps remain almost constant. However, even in the regions of smooth flow, the additional length scale weights larger cells more heavily than small cells, and drives the adaptation process closer toward global refinement.

6. Results

6.1 Validation of Cokriging Method

C_D Optimization for 2-Dimensional Design Case

Two-dimensional Cokriging models were created for the C_D of the supersonic business jet test problem using sample data obtained from CFD analyses. The intent is to validate and investigate the ability of these models to approximate the results of the original CFD code. The two design parameters chosen as were the wing streamwise location along fuselage and the radius of the fuselage at its mid-point. 400 CFD calculations were performed by varying the design variables to obtain a graphical representation of the actual objective functions. The results are shown in Figure 7 (a). The design variables were chosen so as to generate a realistic test function having multiple local extrema to check the ability of Cokriging models to simulate this feature. One important point to note from the Figure is that the actual drag coefficient varies smoothly with respect to the geometric design variables. The selection of Gaussian exponential correlation function for the Kriging method was based on the assumption that

the response function to be modeled was very smooth in nature. Thus, Figure 7 (a) provides the validation of the assumption and the rationale for using the Gaussian correlation function in this problem.

A total of 9 sample points were used to generate the original Kriging model, and the 9 sample points together with gradient information at these points were used for the Cokriging models. From the comparisons in Figure 7, it is clear that Cokriging models performed much better than the Kriging model in predicting both the general shape and magnitude of the objective function. The discrepancies in the original Kriging model are caused by under-sampling.

In order to investigate the applicability of the Cokriging models in 2-dimensional design spaces, C_D optimizations were performed using each of the approximation models generated above. Figure 8 (a) shows the C_D optimization results using the database constructed from 400 CFD calculations over the design space. The optimization used a gradient-based method from Matlab[33] and was repeated five different times by changing the starting points. Four of them converged to one local minimum point and one converged to a different one. The optimizations were again repeated using the different approximation models generated from Kriging and Cokriging methods, and the results are compared in the subsequent figures. As shown, the predicted optimum design point and optimum value of C_D for these cases were nearly identical. The predicted C_D from the CFD database was 0.0059708 whereas those for the Cokriging models with 5 and 9 sample points (and gradients) were 0.0059759 and 0.0059758 respectively with almost the same optimum design point locations. The relative error for the optimized C_D value is within 0.086%. As we can observe from Figure 8 (b), the ability of the original Kriging method to simulate the unknown function was clearly limited without an extensive set of sampled data. The optimum point and the predicted C_D value were far off from the actual ones.

Boom Optimization for 2-Dimensional Design Case

The procedure used in the previous section was repeated for ground boom minimization with a different set of design variables. This time, the design variables and their range of variation were specifically selected to present a challenging boom minimization case. The two design variables selected represent the radii of two fuselage sections located at 10% and 20% of the length of the fuselage. A total of 121 CFD calculations were carried out and the results of the boom strength variation over the design space are shown in Figure 9 (a). Unlike the C_D objective function case, the values of the initial shock jump at the ground vary almost linearly with each design variable until sharp discontinuities are found for lower values of both design variables. This kind of functional variation is considered to be quite difficult to capture with a small number of sample data points. The subsequent Figures show the approximations of the exact boom overpressure values using both Kriging and Cokriging models with 5 sample data points. Similarly to the previous test case, the accuracy of the Kriging model was improved by the addition of gradient information, although the function fits were not as good as in the coefficient of drag case.

Even though Cokriging models had some difficulty to capture the exact variation of the overpressures over the entire design space, three successive design iterations using an empirical trust region methodology produced quite satisfactory results. Figure 10 (a) shows the history of sample points computed for all three design iterations as well as the evolution of the optimum design point superimposed on the exact CFD contour plot (for reference purposes only). Figures 10 (b),(c),(d) represent Cokriging models and the location of the sample points for each design iteration as well as the true and estimated optima for the Cokriging models. After three design iterations the actual location and the function value of the local minimum was achieved fairly accurately.

6.2 Validation of Gradient Enhanced micro-GA

The results of tests of the new hybridization strategy are presented in this section. In Figure 11 (a) (b) we compare the results of the pure micro-GA and gradient enhanced micro-GA algorithms applied to single objective optimization problems on 2-dimensional test functions. The extension of the idea to multiobjective optimization was also tested on 2-D and 10-D test cases and the results are presented in Figure 11 (c) (d). The use of gradient information inside of the GA clearly improves the overall efficiency of the process in terms of the required number of function evaluations to obtain an optimal or sub-optimal solution. GAs have the merit of robustness, implying that they can be used in a wide variety of application problems, but has somewhat poor efficiency in that they require many function evaluations. Gradient-based optimizers, on the other hand, have very high convergence rates but somewhat limited applicability in boom optimization problems. The new idea of hybridization makes it possible to achieve a high level of robustness and efficiency at the same time.

6.3 15-Dimensional Design Problem with QSP107

Multiobjective Optimization using Kriging-Based micro-GAs

Using a latin hypercube sampling technique, 150 sample points around the baseline design point were selected and their performance values were computed using QSP107 calculations. A Kriging model was then generated based on the sampled data and used for the function evaluation routine within the MOGA search. The estimated Pareto set from the Kriging-

based MOGA search procedure is plotted as black circles whereas the CFD validation results of the Pareto set are shown as red asterisks in Figure 12 (a). The results of the MOGA search directly connected to QSP107 for 120 generations are also plotted as blue dots for comparison purposes. The C_D values of the estimated Pareto set from the Kriging-based MOGA and their CFD validation calculations were surprisingly well matched while some of the values of the boom estimations were far off from their CFD counterparts. The results demonstrate the fact that the boom design space may have discontinuous or non-smooth regions and cause difficulties in generating accurate Kriging models. However, the estimation produced some good design points in terms of both design criteria.

One drawback of the Pareto design points was that the ground boom signatures had shapes such that the distance (or time) between the first and second shocks were very small. The outcome implied that the obtained design points were very sensitive to changes in the design variables and would therefore not be acceptable to designers in search of robust designs. The first design iteration described above was repeated with a constraint imposed on the distance between the first and the second peaks of the ground boom signature and its results are presented in Figure 12 (b). Improved Pareto designs (in terms of robustness) were obtained even though the actual values of design criteria did not improve as much as in the previous case.

The second design cycle was performed by collecting another 150 samples around the best designs identified from the previous design cycle, and generating Kriging models for the MOGA search procedure. The results are shown in Figure 12 (c). The estimated Pareto front and the CFD validation results became much closer to each other, as expected, since the design space was restricted for this second iteration.

The resulting design configuration of a point on the Pareto front is compared with that of baseline design in Figure 13. The wing sweep angle, leading edge extension, and dihedral angle increased while the wing position along the fuselage and wing aspect ratio decreased. The nose section was deformed such that it decreased the initial shock strength from the nose and generated an expansion region by inducing a bump-like shape at the lower fuselage section. The effect of this expansion wave is to both weaken the initial shock and to prevent the first and second shocks from coalescing.

Gradient Enhanced Multiobjective Genetic Algorithms (GEMOGA) with Kriging Models

The idea of using Kriging models to provide gradient information to the QSP107-based MOGA in order to accelerate the search procedure was tested using the Kriging models obtained from the first design cycle. The results are presented in Figure 12 (d). As has been demonstrated with analytic test functions, implementing gradient information inside of GA runs greatly improves the convergence rate of the MOGA search and much better Pareto optimal sets could be identified with a smaller number of function evaluations. Furthermore, one can see in this test that Kriging models can provide fairly accurate gradient information at least to assist in the robust search techniques used in the hybrid GAs.

6.4 15-Dimensional Design Problem with QSP-UA

The integration of approximation methods with GAs results in a very robust design optimization framework suitable for typical MDO problems. The technique can effectively be automated and easily adapted to a variety of problems. The bottleneck of the procedure, however, occurs when the mesh perturbation routine fails for configurations requiring a large deviation from the baseline configuration. In addition, the amount of work required to include complex geometry features such as engine nacelles, pylons and diverters, in this environment is rather large. Full automation of the procedure in the context of large geometry perturbations can be achieved with unstructured mesh re-generation and perturbations procedures. If the geometry changes by an amount that would decrease the quality of the volume mesh to the point that it becomes unusable, the mesh can simply be regenerated from scratch. Several measures of mesh quality are readily available in the literature.

The 15-dimensional design problem presented before (with QSP107) was repeated with the QSP-UA environment to demonstrate this new, fully automated, design framework. Function evaluations are computed using the Centaur mesh generation system, the AEROSURF geometry engine, and the AirplanePlus flow solver. Typically, four levels of adaptation are used in each of the function evaluations with mesh sizes in the neighborhood of 3 million nodes.

A total of 140 sample points were initially computed using a Latin Hypercube sampling distribution. The results of these calculations are used to construct Kriging response surfaces which are then fed to our multiobjective GA formulation to arrive at the Pareto front for this problem. The results are very similar to those obtained with the QSP107 multiblock structured approach: the CFD validations of the approximated points on the Pareto front once again appear to show reasonable agreement in the coefficient of drag, but show discrepancies for the calculation of the sonic boom. Once again, this is evidence of the fact that the boom design space is much less smooth than that of the coefficient of drag and, therefore, either larger number of sampling points, or more concentrated sampling locations are needed to improve the accuracy of the fit. Additional iterations with a trust region approach (not computed here) should provide the added

accuracy to achieve closer agreement between the computed and estimated Pareto fronts.

7. Conclusions

The following conclusions can be drawn from the work in this paper:

- Integrated tools for the analysis of sonic boom and aerodynamic performance based on fully nonlinear CFD analyses for both structured and unstructured meshes (QSP107, QSP-UA) have been developed and validated in their applicability to design optimization of low-boom supersonic business jets.

- The applicability and efficiency of approximation model-based GAs has been demonstrated.

- A new hybridization strategy implementing gradient information inside of the GA optimizations was proposed and its advantage to accelerate the GA search procedure has been validated using some preliminary test cases.

8. Acknowledgments

The authors wish to acknowledge the support of the NASA Langley Research Center under Stanford contract number 2DBA401 and the help of Dr. Peter Coen.

References

[1]National Research Council, High Speed Research Aeronautics and Space Engineering Board *Commercial Supersonic Technology : The Way Ahead* , National Academy Press, Washington, D.C., 2002.

[2]Thomas A. Zang and Lawrence L. Green. "Multidisciplinary Design Optimization Technique: Implications and Opportunities for Fluid Dynamics" *30th AIAA Fluid Dynamics Conference*, Norfolk, Virginia, AIAA 99-3798, June 1999

[3]Jaroslaw Sobieszczanski-Sobieski and Raphael T. Haftka "Multidisciplinary Aerospace Design Optimization: Survey of Recent Developments," *34th AIAA Aerospace Sciences Meeting and Exhibit* , Reno, Nevada, AIAA 96-0711, January 1996.

[4]J. Martin, J. J. Alonso and J. Reuther "High-Fidelity Aero-Structural Design Optimization of a Supersonic Business Jet," *43rd AIAA/ASME/ASCE/AHS/ASC Structures, Structural Dynamics, and Materials Conference*, AIAA 2002-1483, Denver, CO, April 2002.

[5]J. Martin and J. J. Alonso "Complete Configuration Aero-Structural Optimization Using a Coupled Sensitivity Analysis Method," *9th AIAA/ISSMO Symposium on Multidisciplinary Analysis and Optimization*, AIAA 2002-5402 Atlanta, GA, September 2002.

[6]Resit Unal, Roger A. Lepsch, Jr. and Mark L. McMillin "Response Surface Model Building and Multidisciplinary Optimization Using Overdetermined D-Optimal Designs," *7th AIAA/USAF/NASA/ISSMO Symposium on Multidisciplinary Analysis and Optimization*, AIAA 98-4759, September 1998

[7]Anthony A. Giunta and Layne T. Watson "A Comparison of Approximation Modeling Techniques: Polynomial Versus Interpolating Models," *7th AIAA/USAF/NASA/ISSMO Symposium on Multidisciplinary Analysis and Optimization* , St. Louis, Missouri, AIAA 98-4758, September 1998.

[8]J. Sacks, W. J. Welch, T. J. Michell, and H. P. Wynn "Design and Analysis of Computer Experiments," *Statistical Science Vol 4. No.4*, pp. 409-453, 1989

[9]Timothy W. Simpson, Timothy M. Mauery, John J. Korte and Farrokh Mistree "Comparison of Response Surface and Kriging Models in the Multidisciplinary Design of an Aerospike Nozzle," *7th AIAA/USAF/NASA/ISSMO Symposium on Multidisciplinary Analysis and Optimization*, St. Louis, Missouri, AIAA 98-4755, September 1998

[10]D. E. Goldberg *Genetic Algorithms for search, optimization, and machine learning*, Addison-Wesley, MA, 1989.

[11]W. Liu and S. Batill "Gradient-Enhanced Response Surface Approximations Using Kriging Models," *9th AIAA/ISSMO Symposium on Multidisciplinary Analysis and Optimization*, AIAA 2002-5456, Atlanta, GA, September 2002.

[12]J. R. Koehler and A. B. Owen "Computer Experiments," *Handbook of Statistics Vol. 13*, pp. 261-308, Elsevier Science, New York, eds. S. Ghosh and C. R. Rao

[13]Edward H. Isaaks and R. Mohan Srivastava *An Introduction to Applied Geostatistics*, Oxford Univ. Press, Oxford, 1989.

[14]H. Chung and J. J. Alonso "Using Gradients to Construct Cokriging Approximation Models for High-Dimensional Design Optimization Problems," *40th AIAA Aerospace Sciences Meeting and Exhibit*, AIAA 2002-0317, Reno, NV, January 2002.

[15]H. Chung and J. J. Alonso "Design of a Low-Boom Supersonic Business Jet Using Cokriging Approximation Models," *9th AIAA/ISSMO Symposium on Multidisciplinary Analysis and Optimization*, AIAA 2002-5598, Atlanta, GA, September 2002.

[16]C. A. Coello Coello and G. T. Pulido "A Micro-Genetic Algorithms for Multiobjective Optimization," *Proceedings of the Genetic and Evolutionary Computation Conference (GECCO'2001)* , 2001.

[17]K. Krishnakumar "Micro-genetic algorithms for stationary and non-stationary function optimization," *SPIE Proceedings : Intelligent Control and Adaptive Systems, pages 289-296*, 1989.

[18]D. L. Carroll "Fortran Genetic Algorithm Driver," *http://cuaerospace.com/carroll/ga.html*, 2001

[19]J. J. Alonso, J. R. R. A. Martins, J. J. Reuther, R. Haimes, and C. A. Crawford "High-Fidelity Aero-Structural Design Using a Parametric CAD-Based Model," *16th AIAA Computational Fluid Dynamics Conference*, AIAA 2003-3429, Orlando, FL., 2003.

[20]J. J. Reuther, J. J. Alonso, J. C. Vassberg, A. Jameson and L. Martinelli. An Efficient Multiblock Method for Aerodynamic Analysis and Design on Distributed Memory Systems. *AIAA Paper 97-1893,* AIAA Fluid Dynamics Conference. Snowmass, CO. June 1997.

[21]James J. Reuther, Antony Jameson, and Juan J. Alonso "Constrained Multipoint Aerodynamic Shape Optimization Using an Adjoint Formulation and Parallel Computers, Parts I and II," *Journal of Aircraft* Vol 36, No 1, January-February, 1999

[22]Kenneth J. Plotkin "PCBoom3 Sonic Boom Prediction Model-Version 1.0e," *Wyle Research Report WR 95-22E*, October. 1998.

[23]Hamies, R. and Follen, G. "Computational Analysis Programming Interface," *Proceedings of the 6th International Conference on Numerical Grid Generation in Computational Field Simulations*, Greenwich, 1998

[24] *Gridgen User Manual ver.13*, Pointwise, Inc., Bedford, 1998

[25] *Centaur System Users' Manual*, *http://www.centaursoft.com*

[26]D. J. Mavriplis. Unstructured Mesh Generation and Adaptivity *ICASE 95-26*

[27]J. Peraire, M. Mahdati, K. Morgan and O. C. Zienkienwicz Adaptive Remeshing for Compressible Flow Computation *Journal of Computational physics, 72:449-466* October, 1987

[28]A. Jameson, T. J. Baker and N. P. Weatherill. Calculation of Inviscid Transonic Flow over a Complete Aircraft. *AIAA*

Paper 86-0103, 24th Aerosapce Sciences Meeting, January 6-9, 1986, Reno, Nevada

[29]T. J. Baker. Mesh Adaptation Strategies for Problems in Fluid Dynamics. *Finite Elements in Analysis and Design*, Vol. 25, 1997, pp. 243-273.

[30]M. A. Park. Adjoint-Based, Three-Dimensional Error Prediction and Grid Adaptation. *32nd Fluid Dynamics Conference*, June 24-27, 2002, St. Louis, MO

[31]R. Lohner. Generation of Unstructured Grids Suitable for RANS Calculations *AIAA Paper 99-0662*, 1999

[32]G. Warren, W. K. Anderson, J. L. Thomas and S. L. Krist Grid Convergence for Adaptive Methods *AIAA paper 91-1592*, June 1991

[33] *Optimization Toolbox For Use with MATLAB, Version 2*, The MathWorks, Inc. Mass., July, 2002

[34]J. J. Alonso, I. M. Kroo and A. Jameson Proceedings of the DARPA QSP Technical Exchange Meeting 5. December 2001.

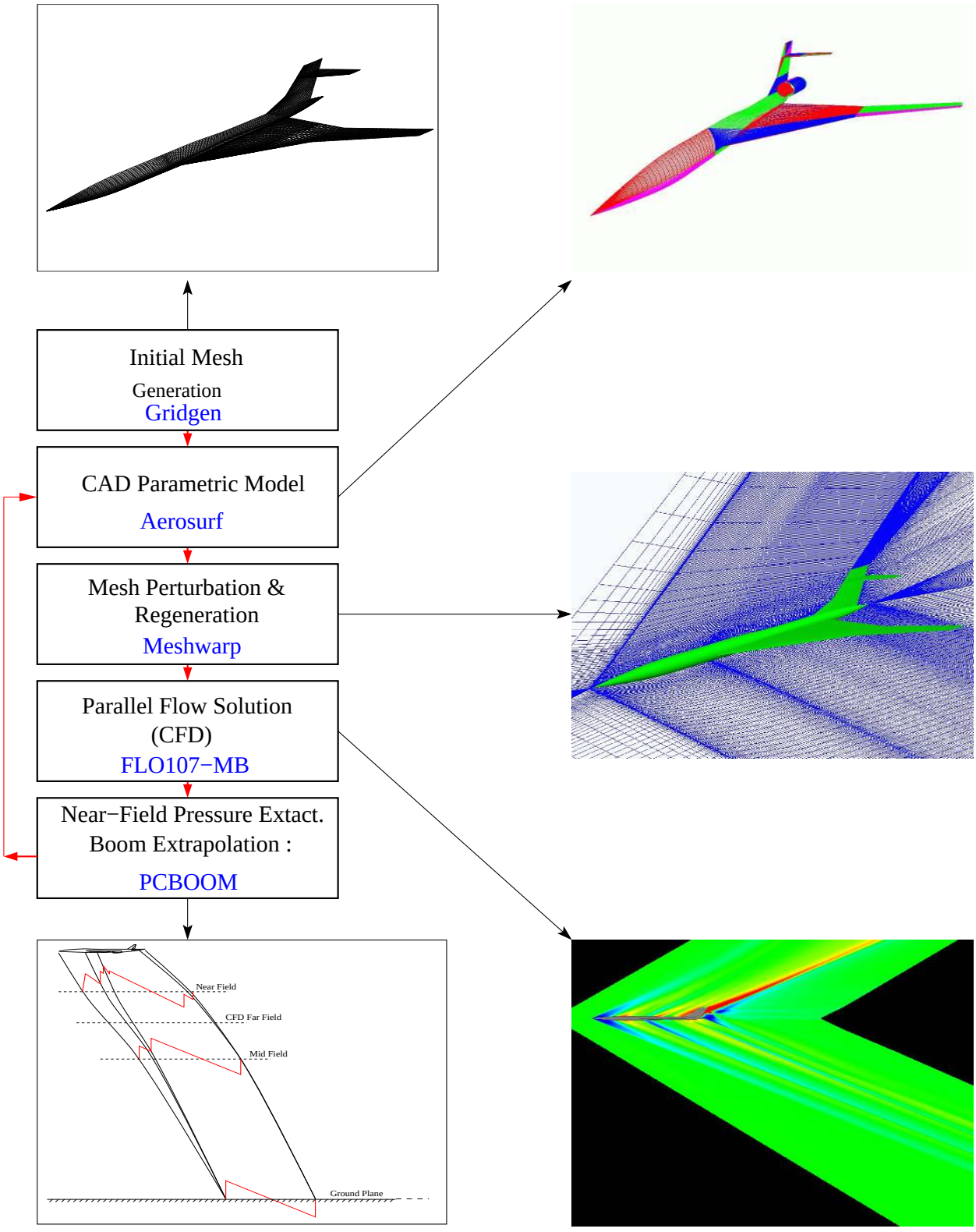

Fig. 5 Flowchart of the Various Modules of the QSP107 Design Tool

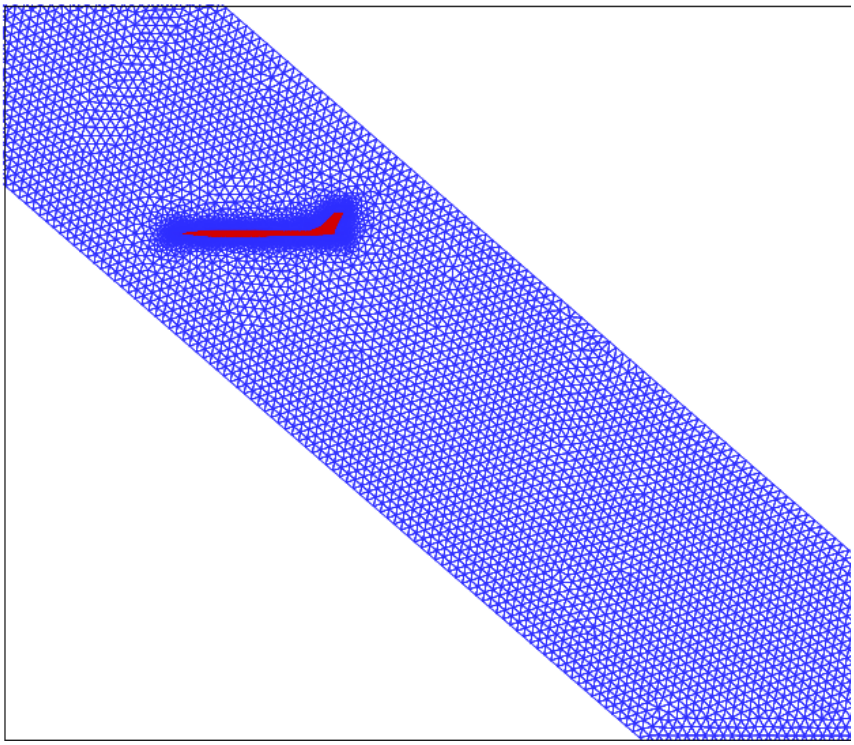

(a) Mesh after first adaptation with number of mesh nodes=562,057

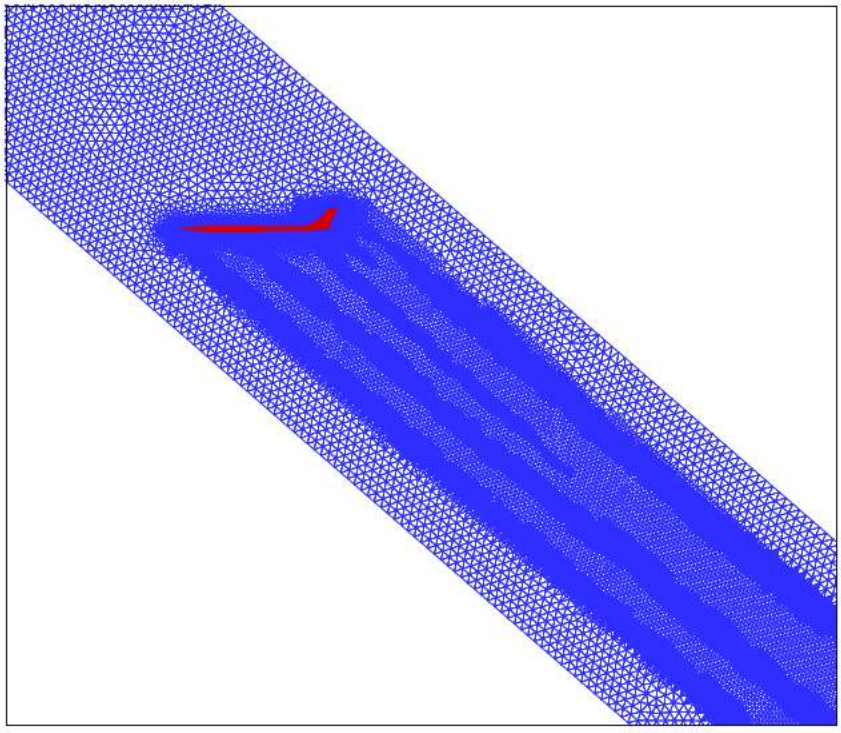

(b) Mesh after second adaptation with number of mesh nodes=1,028,577

Fig. 6 Unstructured Mesh Adaptation for 15-Dimensional SBJ Design Problem

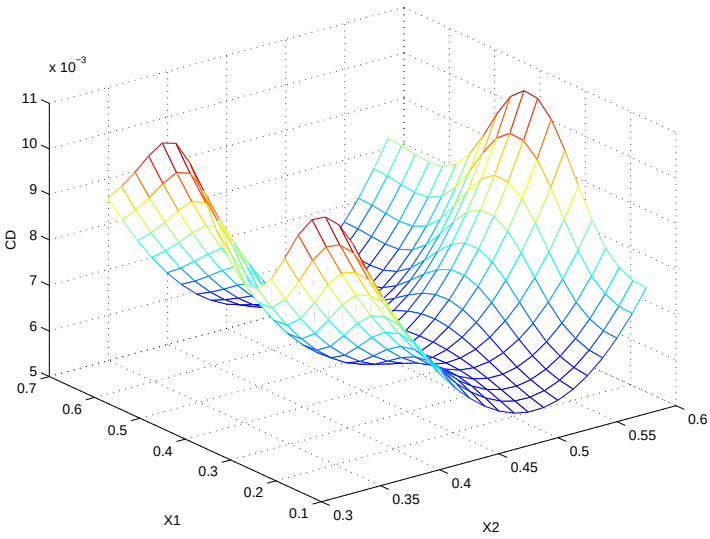

(a) Results of CFD Calculations over 400 Design Points

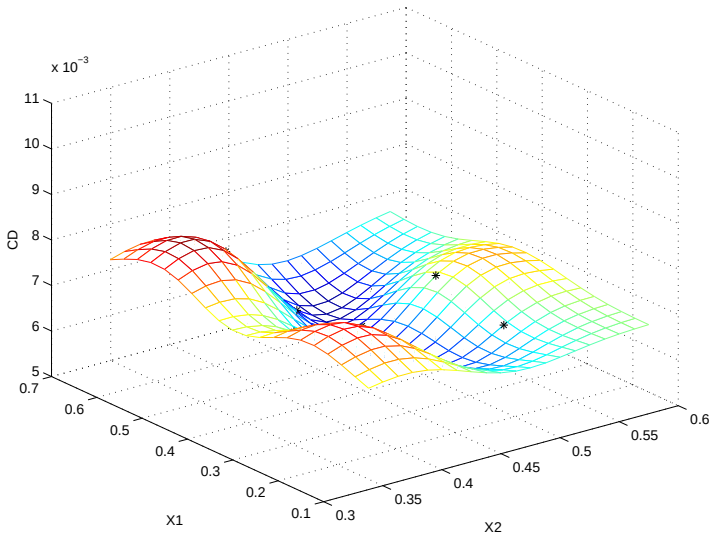

(b) Original Kriging Model with 9 Sample Values

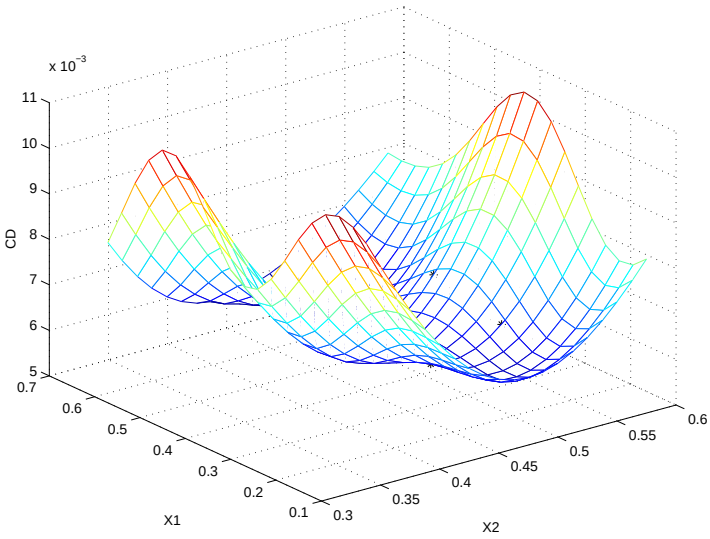

(c) Direct Cokriging Model with 9 Sample Values and their Gradients

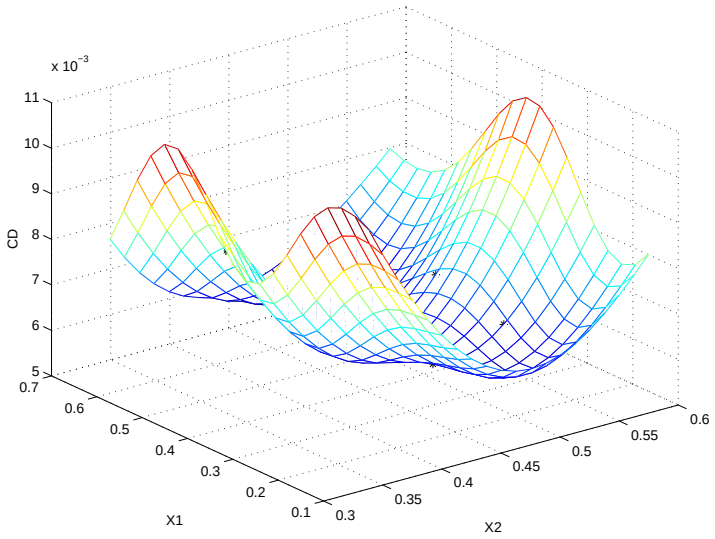

(d) Indirect Cokriging Model with 9 Samples and 18 Additional Values Obtained from Gradients

Fig. 7 Validation Problem. C_D Cokriging Models for 2-D SBJ Test Case Using Two Design Variables: Wing Position and Fuselage Radius at 50% Location

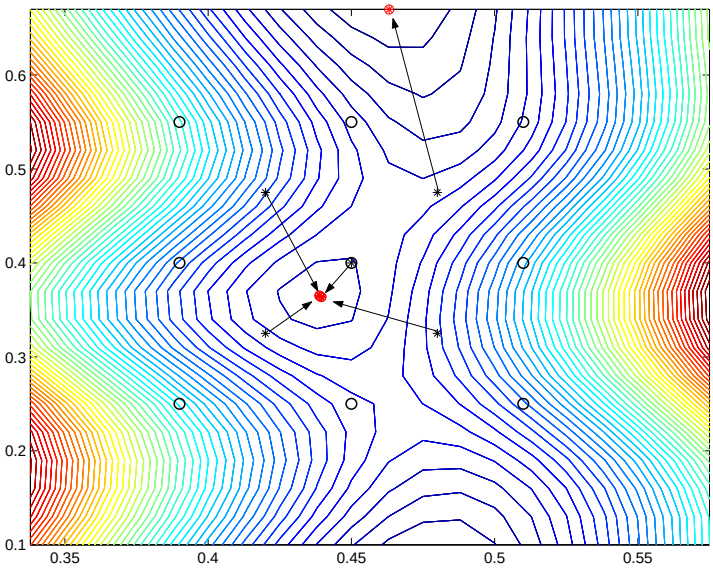

(a) C_D Optimization Using CFD Calculation Results over 400 Design Points

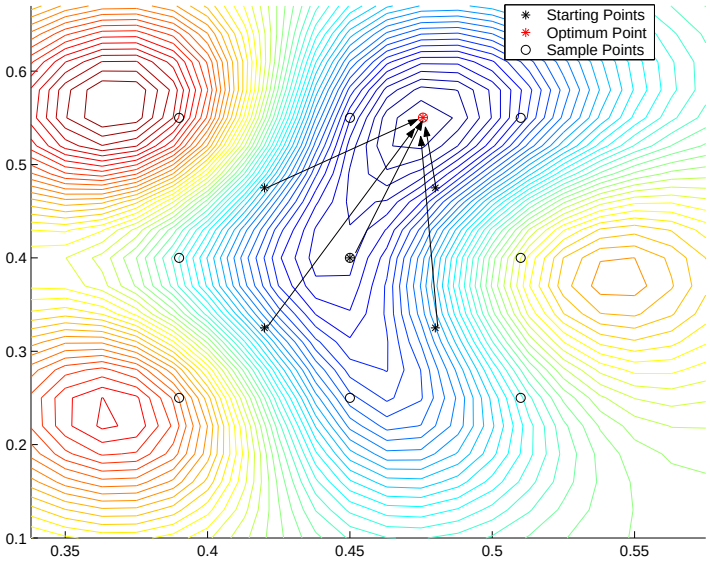

(b) C_D Optimization Using Original Kriging Model with 9 Sample Values

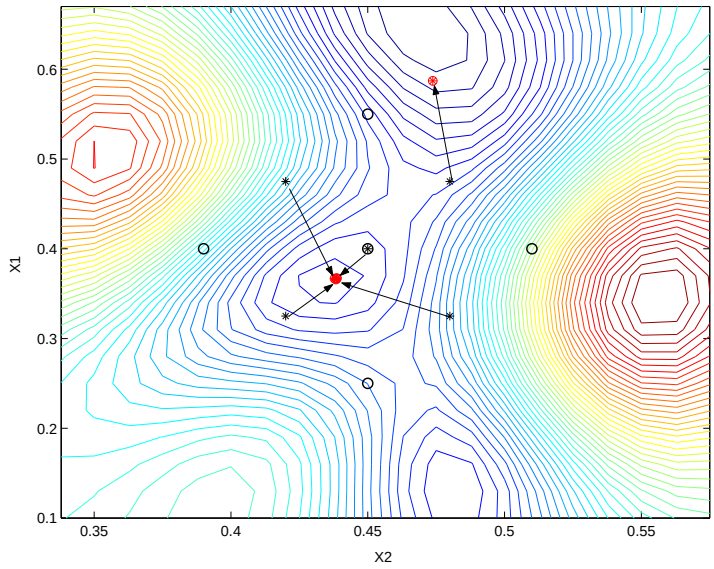

(c) C_D Optimization Using Cokriging Model with 5 Sample Values and their Gradients

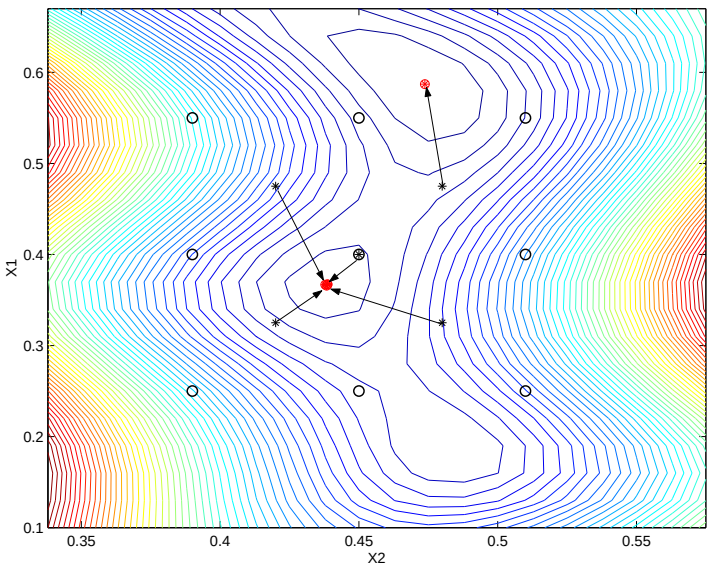

(d) C_D Optimization Using Cokriging Model with 9 Sample Values and their Gradients

Fig. 8 C_D Optimization Results for 2-D SBJ Test Case

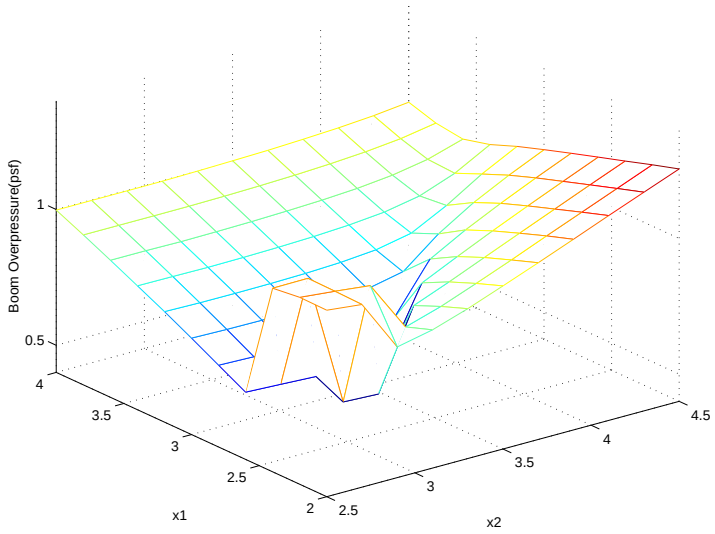

(a) Results of CFD Calculations over 121 Design Points

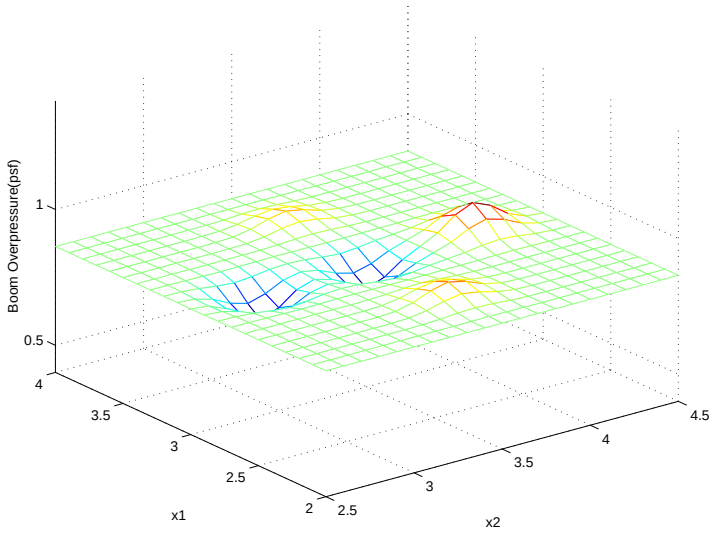

(b) Original Kriging Model with 5 Sample Values

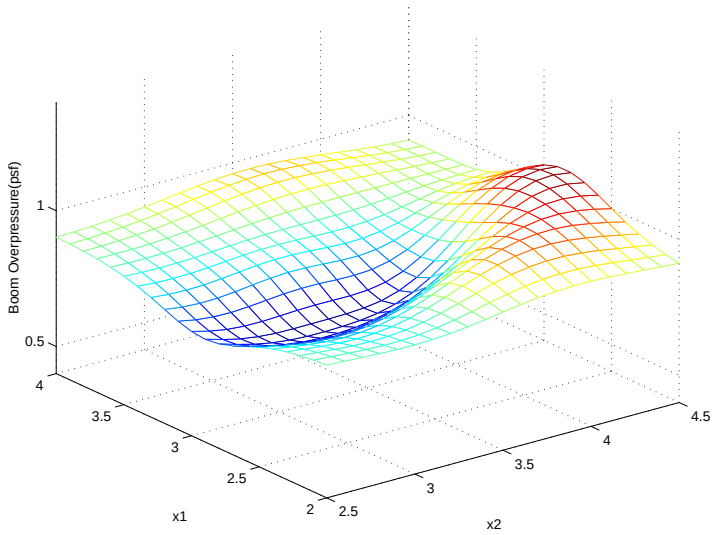

(c) Cokriging Model with 5 Sample Values and their Gradients

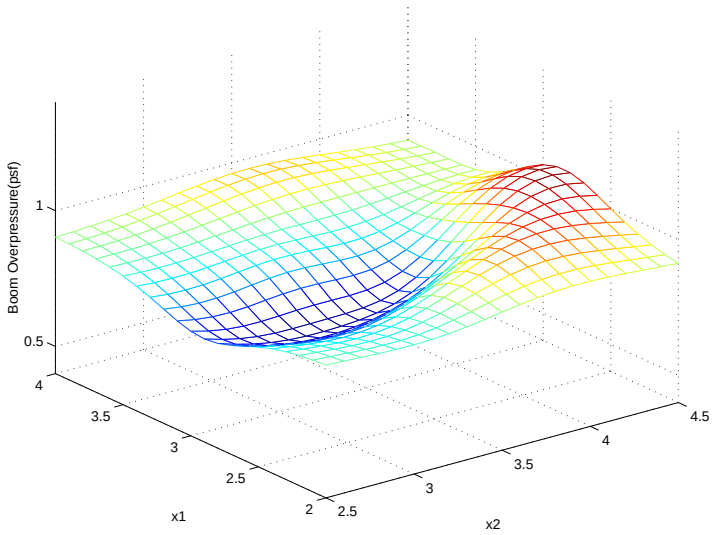

(d) Cokriging Model with 5 Samples and 10 Additional Values Obtained from Gradients

Fig. 9 Boom Overpressure Cokriging Models for 2-D SBJ Design Problem Using Two Design Variables: Fuselage Radii at 10% and 20% Locations

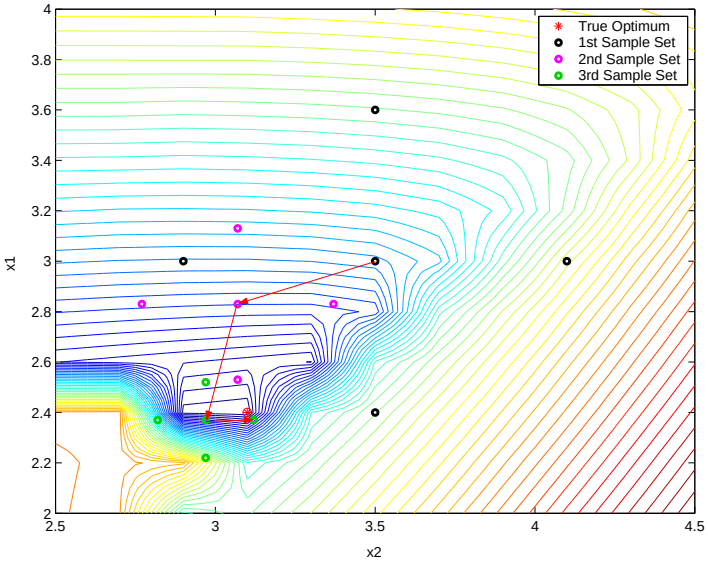

(a) Sample Points Over 3 Design Iterations and Optimum Design Evolution With Contours from CFD Calculations

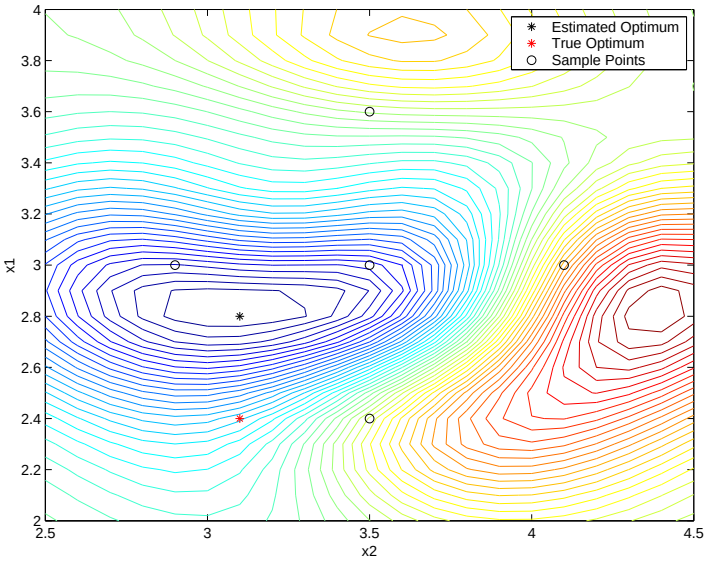

(b) 1^{st} Design Cycle Results with Cokriging Approximation Contour Plot

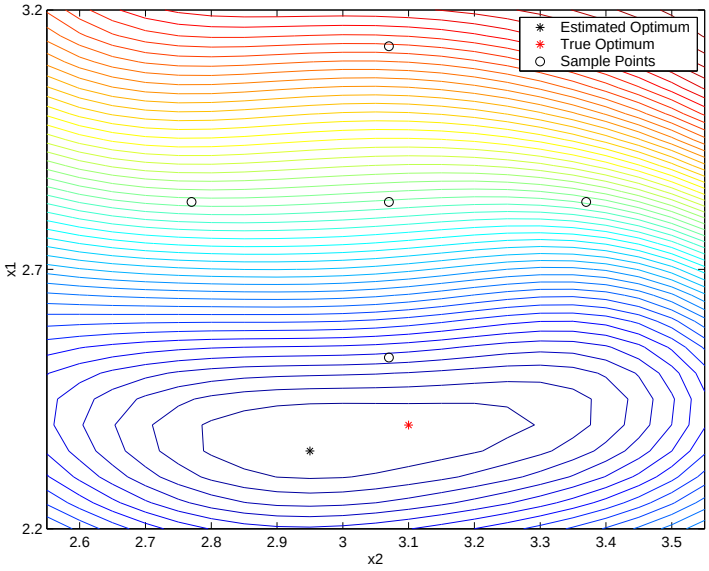

(c) 2^{nd} Design Cycle Results with Cokriging Approximation Contour Plot

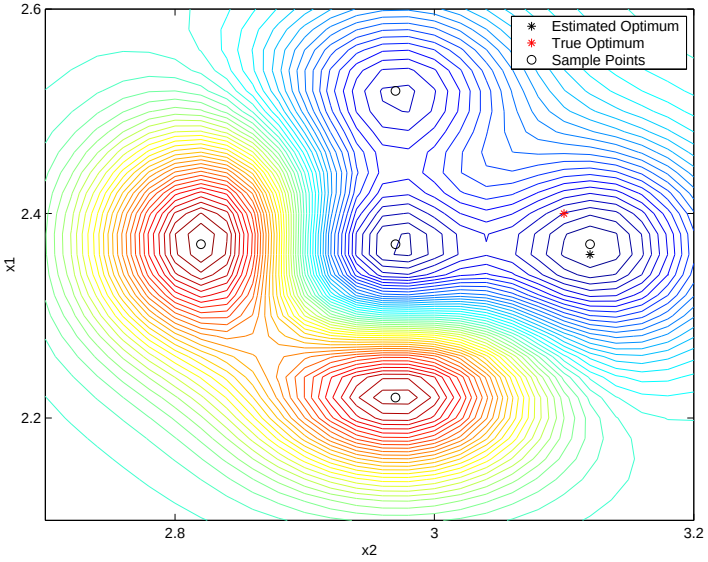

(d) 3^{rd} Design Cycle Results with Cokriging Approximation Contour Plot

Fig. 10 Boom Overpressure Optimization Results using Indirect Cokriging Method for 2-D SBJ Design Problem

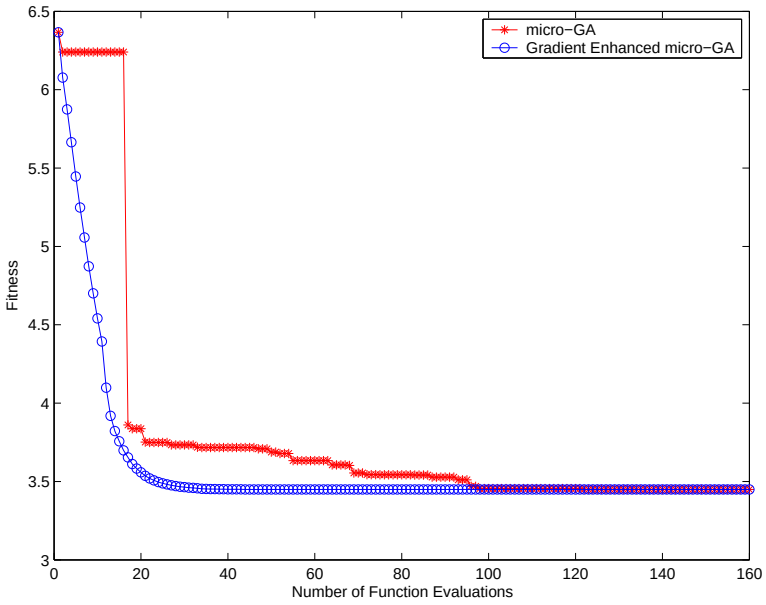

(a) Peaks Test Function (2-D)

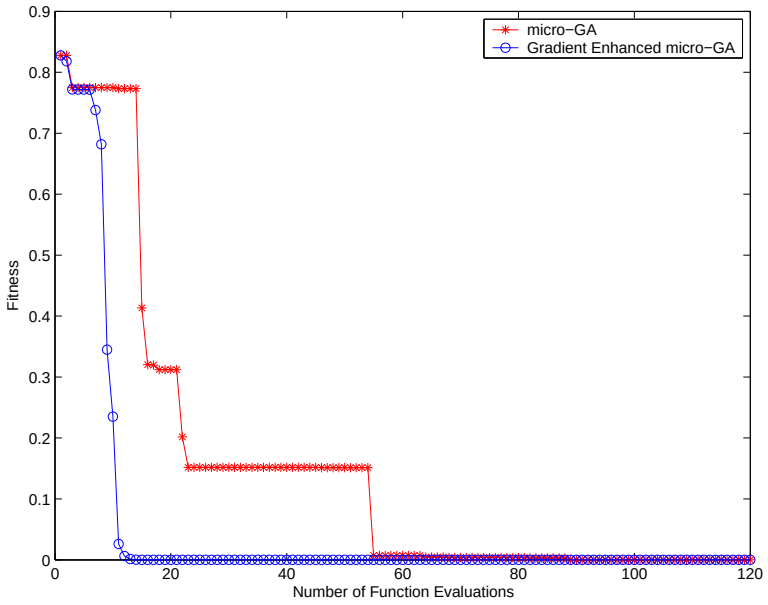

(b) Goldberg's Test Function (2-D)

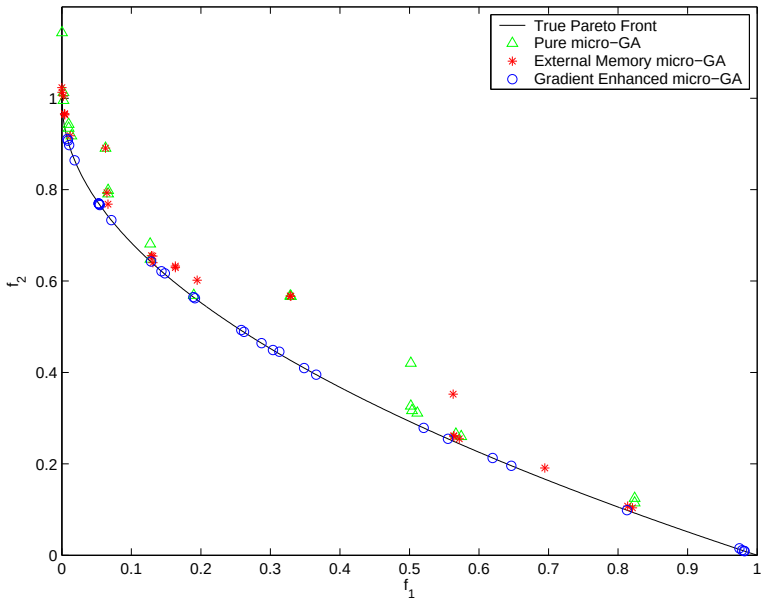

(c) 2-D Multiobjective Test Function

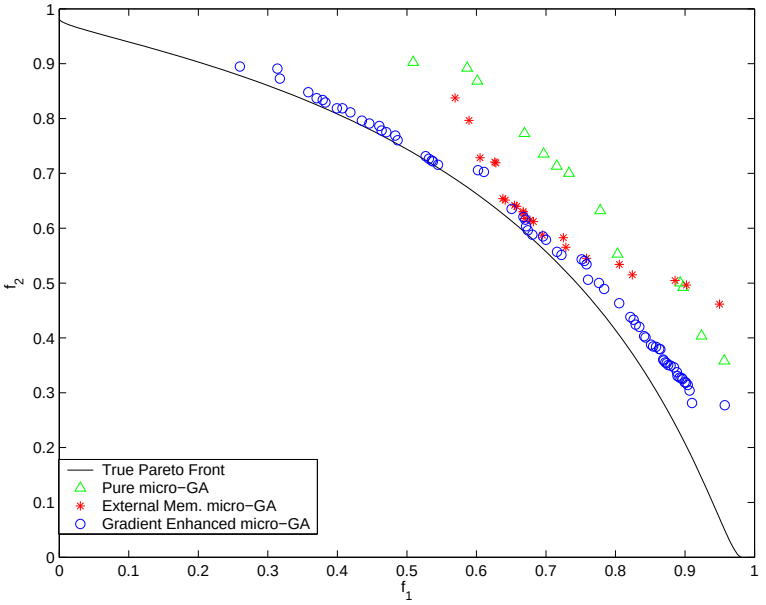

(d) 10-D Multiobjective Test Function

Fig. 11 Validation of Gradient Enhanced micro-GA

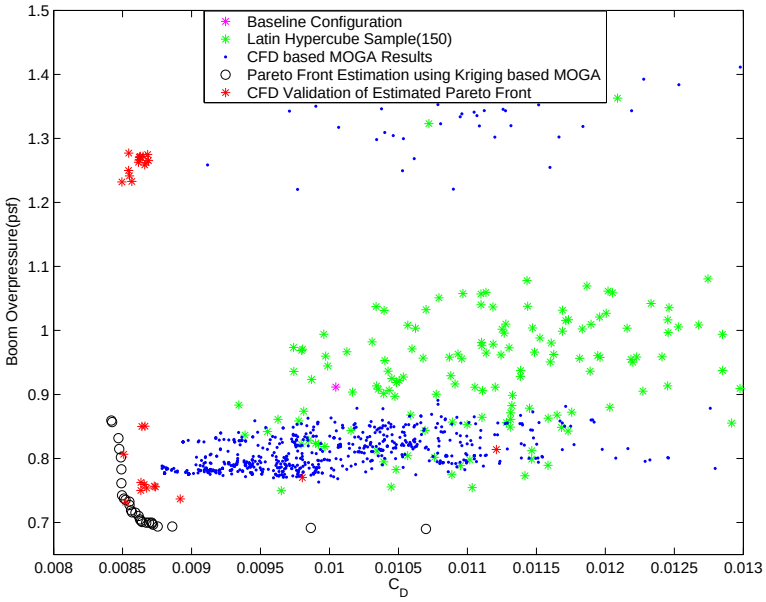

(a) 1^{st} Design Cycle Results using Kriging-Based MOGA without Booom Constraint

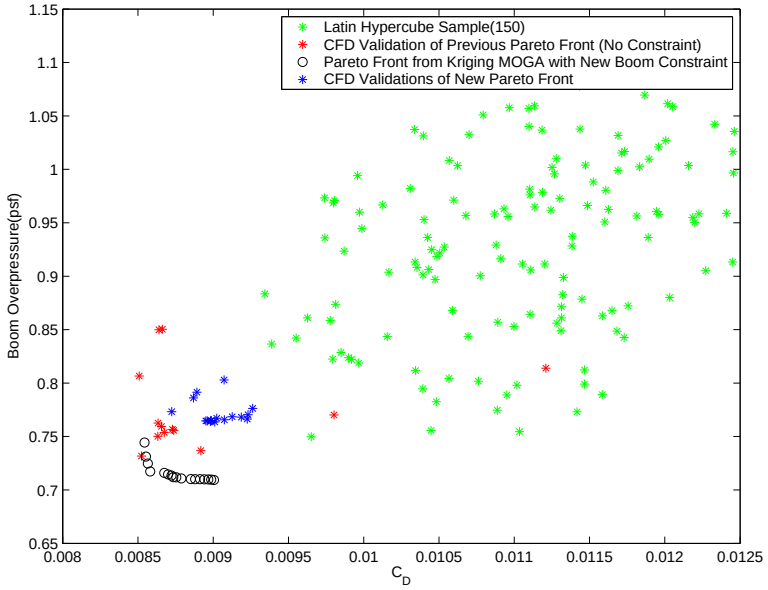

(b) 1^{st} Design Cycle Results using Kriging-Based MOGA with Booom Constraint

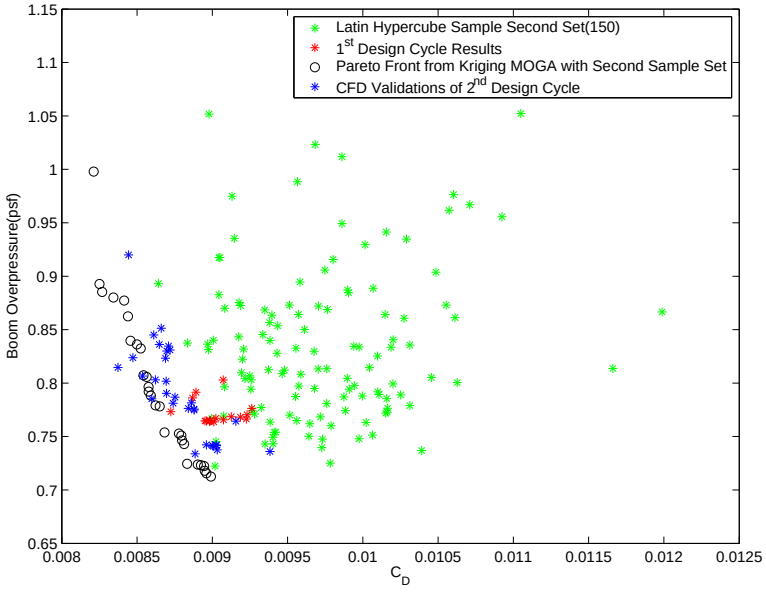

(c) 2^{nd} Design Cycle Results using Kriging-Based MOGA

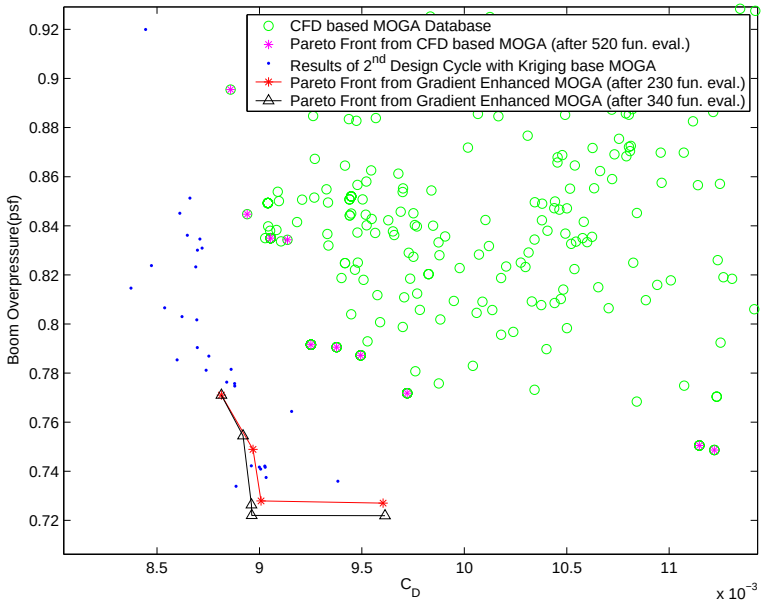

(d) Design Results using GEMOGA with Kriging Models

Fig. 12 Multiobjective Optimization Results

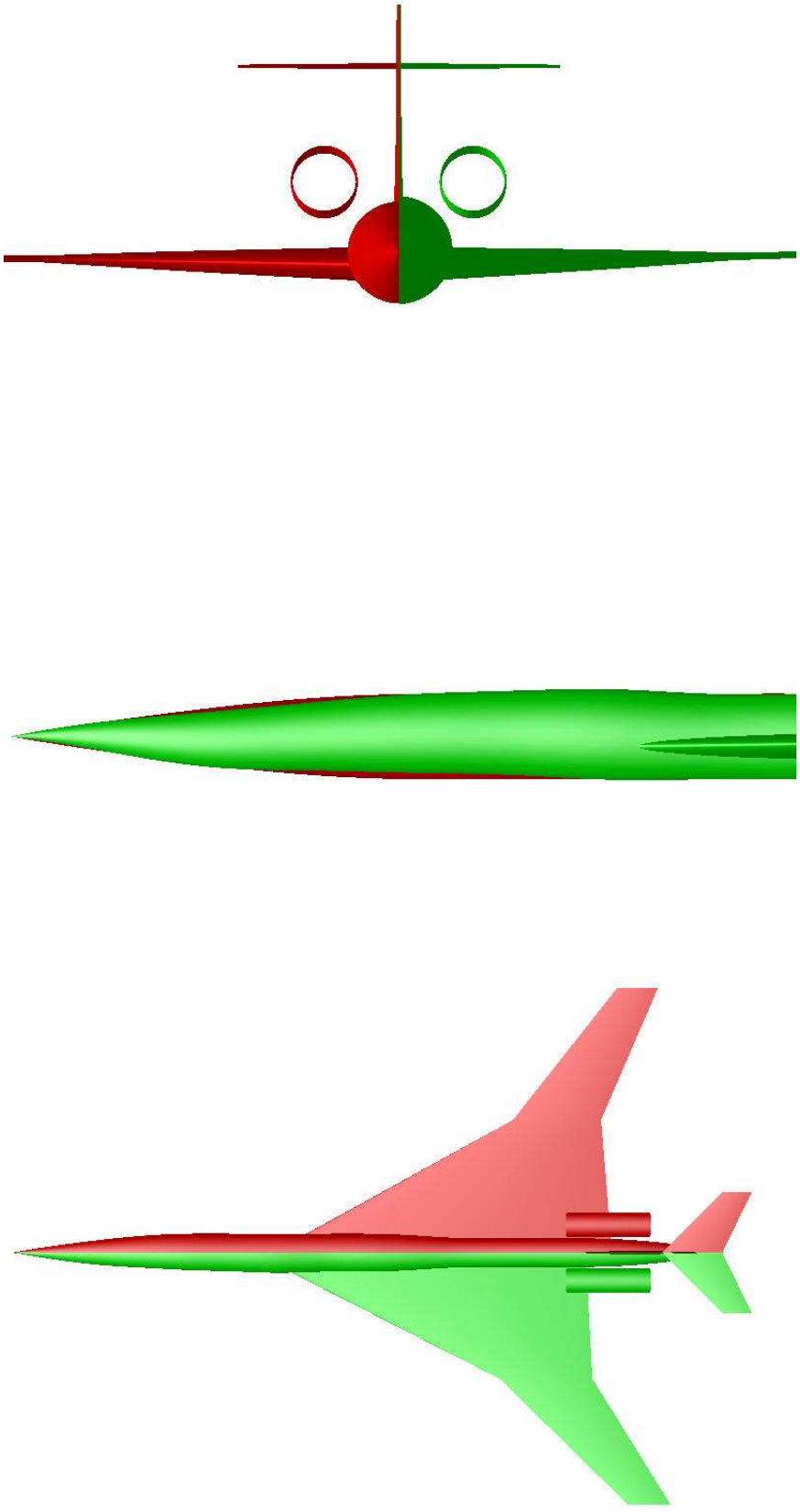

Fig. 13 Configuration Comparison between Final and Baseline Designs (red:baseline, green:Desinged)

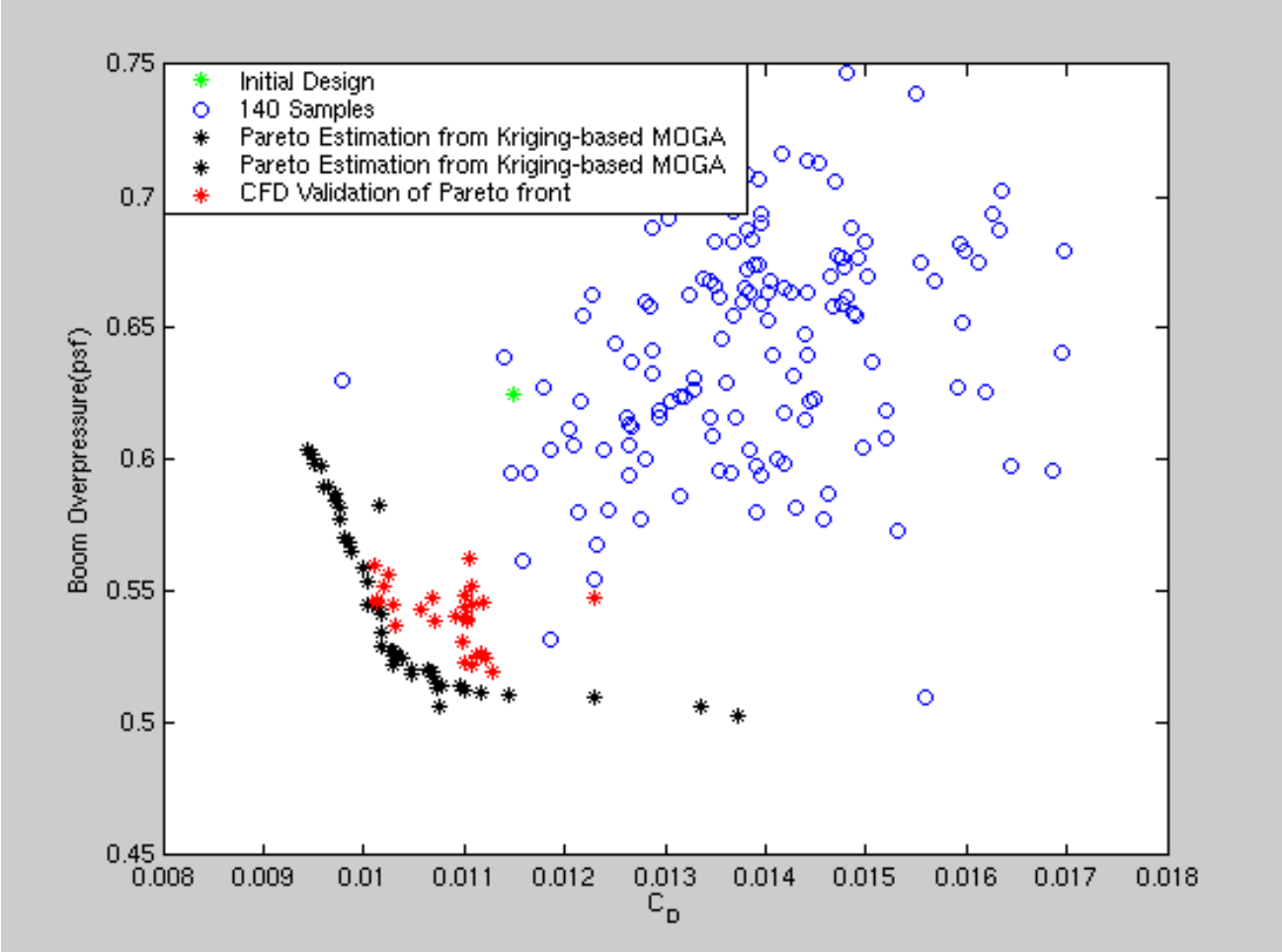

Fig. 14 Results of MOGA using QSP-UA analyses and a Kriging approximation model.